Polycomb-like 2 Associates with PRC2 and Regulates Transcriptional Networks during Mouse Embryonic Stem Cell Self-Renewal and Differentiation

Emily Walker,[1] Wing Y. Chang,[1] Julie Hunkapiller,[4] Gerard Cagney,[5,6] Kamal Garcha,[1] Joseph Torchia,[7] Nevan J. Krogan,[5] Jeremy F. Reiter,[4] and William L. Stanford[1,2,3,8,*]

[1]Institute of Biomaterials and Biomedical Engineering, University of Toronto, Toronto, ON M5S 3G9, Canada
[2]Institute of Medical Sciences, University of Toronto, Toronto, ON M5S 1A8, Canada
[3]Department of Chemical Engineering and Applied Chemistry, University of Toronto, Toronto, ON M5S 3E5, Canada
[4]Department of Biochemistry and Biophysics, Cardiovascular Research Institute
[5]Department of Cellular and Molecular Pharmacology, California Institute for Quantitative Biomedical Research
University of California San Francisco, San Francisco, CA 94158, USA
[6]Conway Institute, University College Dublin, Belfield, Dublin 4, Ireland
[7]Department of Oncology and Biochemistry, London Regional Cancer Program, The Lawson Health Research Institute and the University of Western Ontario, London, ON N6A 4L6, Canada
[8]Institute for Systems Biology, Seattle, WA 98103, USA
*Correspondence: william.stanford@utoronto.ca
DOI 10.1016/j.stem.2009.12.014

SUMMARY

Polycomb group (PcG) proteins are conserved epigenetic transcriptional repressors that control numerous developmental gene expression programs and have recently been implicated in modulating embryonic stem cell (ESC) fate. We identified the PcG protein PCL2 (polycomb-like 2) in a genome-wide screen for regulators of self-renewal and pluripotency and predicted that it would play an important role in mouse ESC-fate determination. Using multiple biochemical strategies, we provide evidence that PCL2 is a Polycomb Repressive Complex 2 (PRC2)-associated protein in mouse ESCs. Knockdown of *Pcl2* in ESCs resulted in heightened self-renewal characteristics, defects in differentiation, and altered patterns of histone methylation. Integration of global gene expression and promoter occupancy analyses allowed us to identify PCL2 and PRC2 transcriptional targets and draft regulatory networks. We describe the role of PCL2 in both modulating transcription of ESC self-renewal genes in undifferentiated ESCs as well as developmental regulators during early commitment and differentiation.

INTRODUCTION

Control over ESC-fate decisions is accomplished through a variety of molecular, genetic, and epigenetic events. Exogenous control of cell fate can be achieved by a limited number of factors. When grown in fetal bovine serum (FBS)-containing medium and in the presence of murine embryonic fibroblast feeder cells (Evans and Kaufman, 1981; Martin, 1981) or the cytokine leukemia inhibitory factor (LIF) (Smith et al., 1988; Smith

and Hooper, 1987; Williams et al., 1988), mouse ESCs remain undifferentiated. BMP4, provided by the serum, functions in the presence of LIF to maintain pluripotency by inducing phosphorylation and nuclear localization of Smad1, followed by upregulation of Id proteins that block neural differentiation (Ying et al., 2003a).

Three transcription factors are known to be critical in the establishment and/or maintenance of ESC pluripotency. OCT4 (*Pou5f1*) has a highly conserved role in maintaining pluripotent cell populations (Morrison and Brickman, 2006; Nichols et al., 1998), and its expression level dictates ESC fate (Niwa et al., 2000). SOX2 forms a complex with OCT4 and is necessary to cooperatively activate target genes (Ambrosetti et al., 1997; Yuan et al., 1995). NANOG is critical for initiating pluripotency and maintaining OCT4 levels, even in the absence of LIF (Chambers et al., 2003; Chambers et al., 2007; Mitsui et al., 2003), while it is itself regulated by OCT4 and SOX2 (Rodda et al., 2005).

The polycomb group (PcG) proteins, first described in *D. melanogaster*, regulate epigenetic states and are required for proper repression of homeotic genes during development (Schuettengruber et al., 2007; Schwartz and Pirrotta, 2007). PcG proteins have been identified in either the PRC1 or the PRC2 multiprotein complex (Lund and van Lohuizen, 2004). The core components of PRC2 in *Drosophila* are Extra Sex Combs, E(Z), and SU(Z)12. These proteins are found in distinct complexes with additional accessory proteins that undergo dynamic changes during development (Furuyama et al., 2003; Kuzmichev et al., 2005). Core PRC2 members are highly conserved between species (Schuettengruber et al., 2007), and their mouse orthologs are EED, EZH2, and SUZ12, respectively (Cao et al., 2002; Czermin et al., 2002). Through the methyltransferase activity of EZH2, PRC2 induces gene repression by trimethylating lysine 27 on histone 3 (3meH3K27) (Cao et al., 2002; Pasini et al., 2004; Silva et al., 2003).

In *Drosophila*, PCL (polycomb-like) is present in a subset of PRC2 complexes (O'Connell et al., 2001; Tie et al., 2003). Evidence suggests that PCL is required to generate high levels
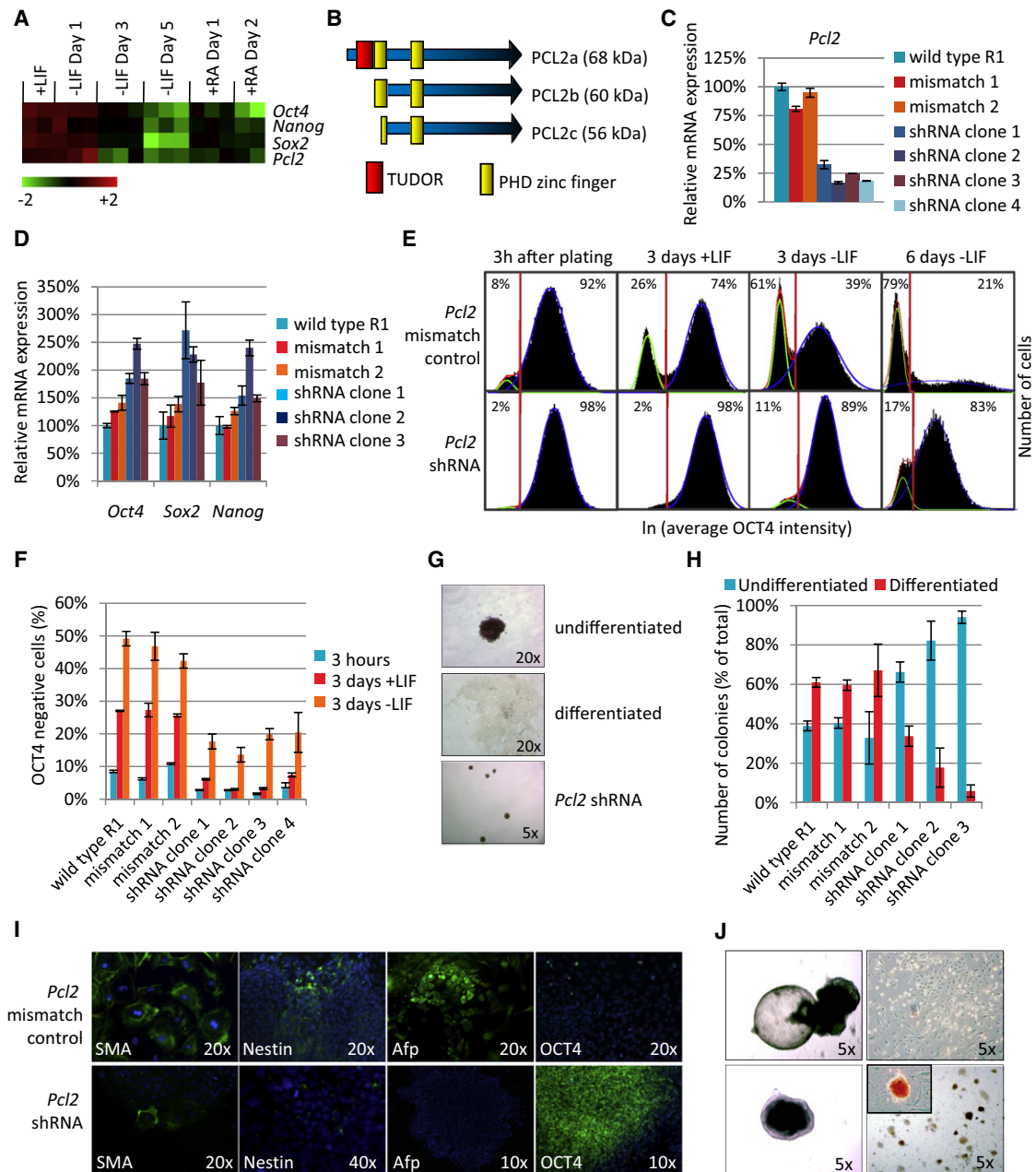
Figure 1. Downregulation of *Pcl2* Leads to Enhanced Self-Renewal and Impaired Differentiation Capacity

(A) Microarray expression profile of *Pcl2* throughout both −LIF and +RA monolayer differentiation of OCT4:eGFP R1 ESCs.

(B) PCL2 has three predicted isoforms.

(C) Relative expression of *Pcl2* mRNA in control and shRNA knockdown clones. Data are presented as mean ± standard deviation of triplicate experiments.

(D) Relative expression of *Oct4*, *Nanog*, and *Sox2* in three different *Pcl2* shRNA knockdown clones compared to wild-type R1 and two mismatch controls as determined by qPCR. Data are presented as mean ± standard deviation of triplicate experiments.

(E and F) OCT4 protein was measured by quantitative immunofluorescence in 10,000 individual cells of three different *Pcl2* shRNA knockdown clones over 72 hr in both +LIF and −LIF conditions. In (E), the distribution of OCT4 expression is illustrated in a histogram for one representative *Pcl2* shRNA knockdown clone and a mismatch control. The distribution is best modeled as a double-Gaussian (red curve) which is a compilation of the OCT4-negative population (green curve) and the OCT4-positive population (blue curve). The vertical red line represents the threshold between OCT4 +ve and −ve populations, and the percentage of cells above and below this threshold is reported. In (F), the percentage of cells that had lost OCT4 expression at each time point is reported. Error bars represent the standard deviation of triplicate experiments.

(G and H) Three different *Pcl2* shRNA knockdown clones, wild-type R1, and two mismatch controls were plated in +LIF, and the distribution of colonies on each plate that were undifferentiated or fully differentiated were determined by morphology and alkaline phosphatase (ALP) expression. The results are an average of three separate experiments, each performed in triplicate.

of 3meH3K27 at some target genes. However, gene repression and 3meH3K27 of many known PRC2 targets is not abolished in the absence of PCL, suggesting that PRC2 can function independently of PCL at many target genes (Nekrasov et al., 2007). In contrast to other PRC2 members, the lack of PCL produces a mild homeotic phenotype, specifically affecting target gene expression in central nervous system and mesoderm tissues (Duncan, 1982; O'Connell et al., 2001). PCL2 is a mammalian ortholog of PCL, and defects reported in animal models of *Pcl2* deficiency are consistent with lack of PCL in *Drosophila*. In *G. gallus* (Wang et al., 2004), *Pcl2* regulates left-right axis specification, and in *X. laevis* (Kitaguchi et al., 2001), central nervous system gene expression is disrupted by the lack of *Pcl2*. Finally, hypomorphic *Pcl2* gene trap mice have pleiotropic defects, including posterior transformation of axial skeleton, stunted growth, hydrocephaly, hunchback, and incisor abnormalities (Wang et al., 2007).

Here, we investigated the role of PCL2 in mouse ESCs. Reduction of PCL2 resulted in heightened self-renewal characteristics and inefficient differentiation to the three germ layers. PCL2 was found to associate with the core PRC2 complex, and using chromatin immunoprecipitation (ChIP) coupled with massively parallel DNA sequencing (ChIP-seq), we found that PCL2 is highly enriched at many, but not all, locations of PRC2 enrichment. Loss of PCL2 did not abolish global levels of 3meH3K27 but did result in decreased 3meH3K27 at specific targets and altered patterns of 3meH3K27 during early commitment. Integrating PCL2-PRC2 targets with the ESC self-renewal circuitry revealed a key role for PCL2-PRC2 in limiting transcription of ESC self-renewal genes in undifferentiated ESCs, as well as controlling developmental regulators during commitment and early differentiation.

RESULTS

Identification of Mammalian *Pcl2*

In a screen for regulators of ESC fate, we hypothesized that networks critical for the stability of the ESC state would be differentially regulated at the initiation of commitment (Walker et al., 2007). Transcript levels of *Mtf2* (*metal response element binding transcription factor 2*) decreased during differentiation (Figure 1A), and promoter occupancy data indicated that *Mtf2* is bound by both OCT4 and NANOG (Loh et al., 2006). Further inspection revealed that the protein product of *Mtf2* is orthologous to *Drosophila* PCL. Both proteins contain a TUDOR domain and two PHD zinc finger domains (Figure 1B), and MTF2 shares 73% and 88% similarity to the PCL ortholog, PCL2, studied in *X. laevis* (Kitaguchi et al., 2001) and *G. gallus* (Wang et al., 2004), respectively. The mouse and human MTF2 protein sequences share 96% identity. Thus, we will refer to the mammalian *Mtf2* transcript as *Pcl2.* Mammals have two other PCL orthologs, PHF1 and PHF19, which have 63% homology with PCL2 among the conserved domains. Interestingly, expres-

sion analysis of *Pcl2* in mice shows that it is uniquely expressed in undifferentiated ESCs and during early embryonic development (Figure S1A available online).

Downregulation of *Pcl2* Results in Enhanced Self-Renewal of ESCs

To examine the function of *Pcl2* in ESCs, endogenous *Pcl2* expression was stably knocked down using short hairpin RNA (shRNA) (Kunath et al., 2003). We designed three shRNA sequences targeting different regions of the *Pcl2* mRNA, as well as a mismatch control sequence to rule out indirect effects. One shRNA sequence resulted in the most significant reduction in *Pcl2*. Three of these clones, each exhibiting at least 70% knockdown in *Pcl2* transcript compared to the mismatch control and wild-type R1 ESCs, were chosen for further analysis (Figure 1C) and used in all subsequent experiments. However, stable clones expressing the additional two shRNA sequences were analyzed in many of the assays and showed similar results (data not shown). We also confirmed that knockdown in *Pcl2* mRNA levels resulted in reduced protein levels (Figures S2B and S2C).

To test the effect of *Pcl2* depletion on ESC self-renewal, we measured transcript levels of *Oct4*, *Nanog*, and *Sox2* and found that they were increased in *Pcl2* knockdowns (Figure 1D) over both wild-type and mismatch controls. Next, we performed a high-content fluorescence imaging assay to examine OCT4 protein levels in single cells (Davey and Zandstra, 2006; Walker et al., 2007). The OCT4 distribution is best estimated by a double Gaussian curve, and a threshold delineating OCT4 +ve and −ve cells was calculated as the intersection of these two curves (Davey and Zandstra, 2006). Results are reported as the percentage of cells above and below this threshold. At 3 hours after plating, the cells were viable and contained over 90% OCT4-positive cells (Figure 1E). Cells were cultured under multiple differentiative conditions to study the effects of known self-renewal mediators LIF and BMP4. In all cases, *Pcl2* knockdowns maintained a larger OCT4 +ve population (Figures 1E and 1F, BMP4; data not shown). However, the intensity of the OCT4 +ve peak in knockdown cells was not increased compared to the control (Figure 1E). Thus, individual cells did not overexpress OCT4. Instead, a greater percentage of the population was OCT4 +ve. This resulted in the appearance of overexpression in bulk analyses (Figures 1D and 4A) and highlights the importance of single-cell analyses in distinguishing distinct cell states within a heterogeneous population.

In clonogenic assays (Peerani et al., 2009; Zhang et al., 2006), cultures were stained for alkaline phosphatase (ALP) activity and colonies were stringently scored, with only colonies resembling those in Figure 1G being counted as undifferentiated. *Pcl2* knockdown cells formed undifferentiated colonies with much greater efficiency than controls (Figure 1H). Collectively, these results suggest that knockdown of *Pcl2* promoted self-renewal and maintained the undifferentiated state of ESCs during the initial time points following the cue to differentiate.

(I) Fluorescent images depict *Pcl2* shRNA knockdown and mismatch control cells stained for smooth muscle actin, Nestin, alpha fetoprotein, or OCT4 following EB differentiation. Differentiation experiment was performed in duplicate.

(J) EBs were formed in suspension and cultured for 25 days (left panel). After 25 days, they were trypsinized, cultured in +LIF for 3 days, and stained for ALP (right panel).

Downregulation of *Pcl2* Results in Impaired Differentiation Capacity

To test the effect of *Pcl2* on differentiation capacity, we performed directed neuroectoderm differentiation (Ying et al., 2003b) assays and found *Pcl2* knockdown cells maintained high levels of OCT4 with no observable expression of Nestin within a 5 day period (data not shown). Next, we used embryoid body (EB) formation to determine how the cells would respond when stimulated to differentiate for a prolonged period. Compared to controls, knockdown EBs remained rounded, and in general, cells did not migrate outwards, nor did they acquire a differentiated morphology. Based on immunostaining, control EBs formed large areas of both smooth muscle actin (SMA, mesoderm) and Nestin (neuroectoderm)-positive cells while knockdown EBs formed very few differentiated cells (Figure 1I). Furthermore, knockdown EBs did not form α-fetoprotein (endoderm)-positive cells and maintained high levels of OCT4 expression throughout the cultures (Figure 1I). We also tested whether expression of lineage-specific genes was disrupted and found that although transcripts of some markers of mesoderm and ectoderm were eventually expressed, their expression was delayed (Figure S1B). We also observed that endoderm markers were expressed to different extents in knockdowns compared to controls (Figure S1B).

To test whether knockdown EBs would eventually differentiate after extended culture, EBs were grown in suspension for 25 days (Kaji et al., 2006). After 25 days, control cultures consisted of cystic EBs (Figure 1J, top left) that, when plated on gelatin, developed into cells of differentiated morphology that did not exhibit ALP activity (Figure 1J, top right). In contrast, knockdown EBs remained as small, tightly compacted groups of cells (Figure 1J, bottom left) and retained the capacity to form undifferentiated ALP +ve colonies (Figure 1J, bottom right).

These data suggest that *Pcl2* is critically involved in early commitment and differentiation. Knockdowns appeared unable to progress to terminal differentiation of some cell types and retained a population of self-renewing ESC-like cells.

Ectopic Expression of PCL2 Partially Rescues Knockdown Phenotype

To verify that the phenotype observed was specific to the depletion of *Pcl2*, we performed rescue experiments by ectopically expressing *Pcl2-IRES-βgeo* with a doxycycline-inducible transposon expression system (Woltjen et al., 2009). Clones expressing the transgene encoding the predominate ESC isoforms (Figures S2A and S2B) were selected based on β-galactosidase expression (Figure 2A), PCL2 protein levels (Figure 2B), and *Pcl2* transcript (Figure 2C) following 72 hr of treatment with doxycycline. In colony-forming assays, overexpression of PCL2 was not sufficient to return the normal ratio of differentiated to undifferentiated colonies in +LIF (Figures 2D and 2E). However, under −LIF conditions, rescue clones regained the ability to differentiate (Figure 2E) and contained a normal percentage of OCT4-negative cells (Figure 2F). Finally, after long-term culture in doxycycline, expression of ESC-specific genes *Oct4*, *Sox2*, *Nanog*, *Esrrb*, and *Tcl1* were decreased (Figure 2G). These data demonstrate that following overexpression of *Pcl2* in the knockdown clones, cells recover the ability to downregulate the pluripotency network and differentiate.

PCL2 Is a PRC2-Associated Protein

In *Drosophila*, PCL associates with PRC2 (O'Connell et al., 2001; Savla et al., 2008); therefore, we examined whether murine PCL2 associated with the PRC2 complex. Gel filtration analysis indicated that PCL2 is found in two chromatographically distinct peaks: a large molecular mass peak that coeluted with SUZ12, EZH2, and EED and a smaller peak, which may represent the monomeric form of PCL2 or smaller subcomplexes. SUZ12 and EED were also detected in fractions corresponding to the smaller PCL2 peak (Figure 3A). These associations were confirmed by coimmunoprecipitation experiments (Figure 3B). Previous reports have suggested that PCL2 does not directly interact with EZH2 (O'Connell et al., 2001), which prompted us to further substantiate its association with SUZ12 using a nonbiased epitope-tagged SUZ12 system coupled to mass spectrometry.

We purified SUZ12-associated proteins from a mouse ESC line containing a 6xHis-3xFLAG tag (HF) targeted to the C terminus of one allele of the *Suz12* gene, which resulted in expression of a full-length tagged SUZ12 protein (Singla et al., 2010). SUZ12-associated proteins were then separated by SDS-PAGE and stained with Coomassie blue to identify interacting proteins (Figure 3C). Mass spectrometric analysis indicated that the two prominent bands at approximately 100 and 55 kDa contained proteins SUZ12, EZH1, and EZH2 and RBBP4, RBBP7, AEBP2, EED, and PCL2, respectively (Figure 3D). In addition to a number of previously known interactors of the PRC2 complex including RBBP4, RBBP7, and AEBP2 (Figure 3D) (Kim et al., 2009; Kuzmichev et al., 2002), we identified 15 peptides of PCL2 (Table S1). Taken together, these data demonstrate that PCL2 associates with the PRC2 complex in mouse ESCs.

PCL2 Knockdown Disrupts Global 3meH3K27 during Differentiation

The PRC2 complex is responsible for mediating gene repression by trimethylating H3K27. Loss of the core members of PRC2 results in disruption of the complex and decreased global 3meH3K27. Reduction of PCL2 using shRNA led to moderately increased levels of EZH2 (Figures 4A and 4C) and global 3meH3K27 (Figures 4A and 4D) in the undifferentiated state, while levels of 1meH3K27 were unchanged (Figure 4B). Following LIF withdrawal, EZH2 initially declined, and by day 6, the control cells comprised three distinct cell populations expressing different levels of EZH2 (Figure 4C). In the knockdown cells, EZH2 levels did not decrease during the first 4 days of LIF withdrawal, and a small portion of cells displayed decreased EZH2 at day 6 (Figure 4C). 3meH3K27 levels decreased in both control and knockdown cells immediately following differentiation. Consistent with their undifferentiated state, the knockdown cells had slightly more 3meH3K27 during the first day of differentiation but contained similar levels to the control cells by day 4 of differentiation. At day 6, control cells consisted of two different populations of cells displaying two low but distinct levels of 3meH3K27, whereas knockdown cells comprised a single population (Figure 4D). These data reveal *Pcl2* is dispensable for EZH2 expression and global 3meH3K27 in undifferentiated cells. However, upon the withdrawal of LIF, levels of both EZH2 and 3meH3K27 decline below the levels of the control.
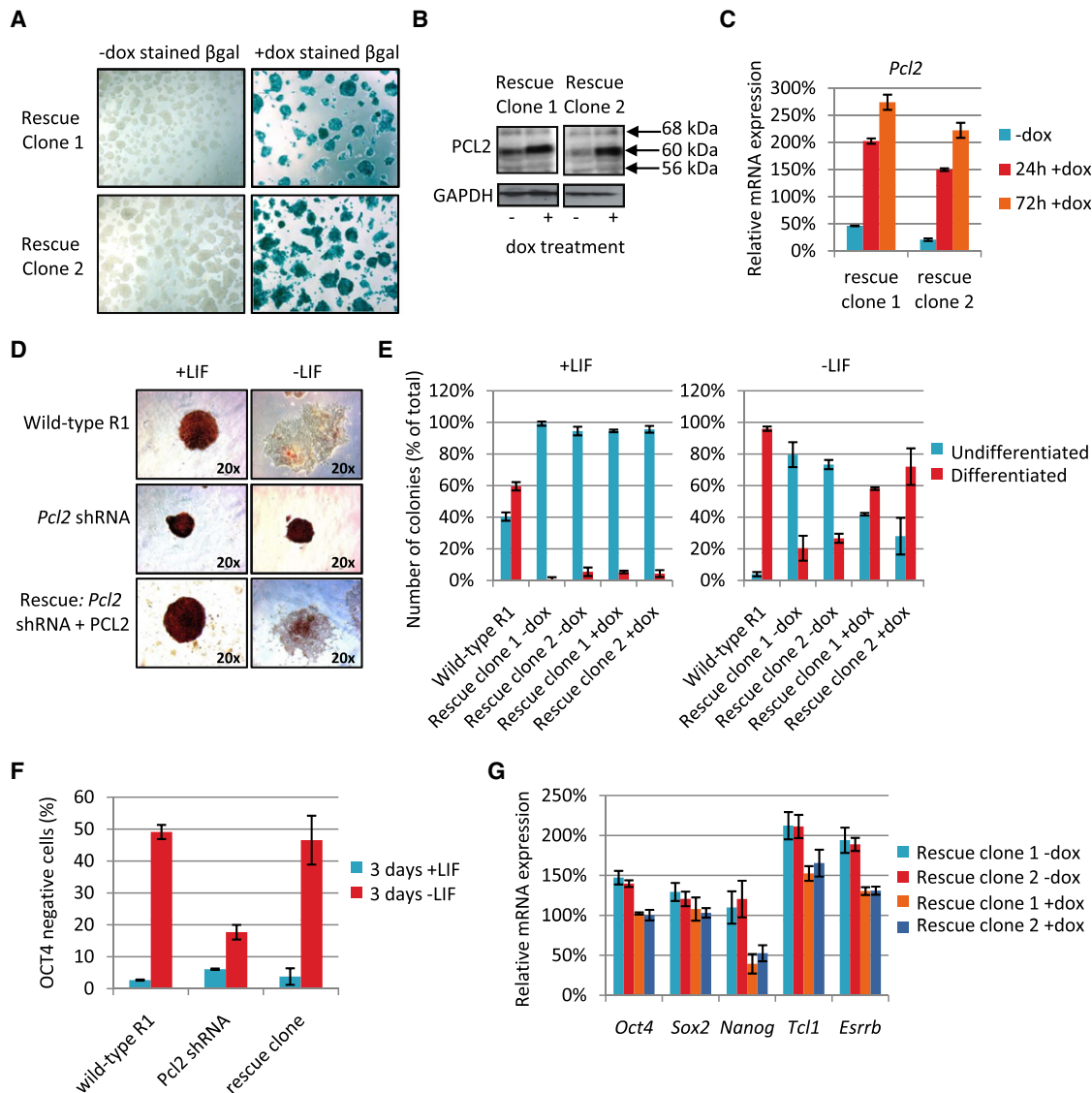
Figure 2. Induced Expression of PCL2 Partially Rescues Knockdown Phenotype

(A) Two *Pcl2* shRNA clones containing the doxycycline inducible *Pcl2-IRES-βgeo* expression cassette were stained for β-galactosidase expression before and 72 hr after addition of doxycycline to the media.

(B) By western analysis, PCL2 protein was increased in the two rescue clones following doxycycline induction.

(C) By qPCR analysis, *Pcl2* transcript was increased following doxycycline induction. Data are presented as mean ± standard deviation of triplicate experiments.

(D and E) The rescue clones were plated in +LIF or −LIF, with or without doxycycline, and the distribution of colonies on each plate that were undifferentiated or fully differentiated were determined by morphology and alkaline phosphatase (ALP) expression. Data are presented as mean ± standard deviation of triplicate experiments.

(F) The percentage of cells in the rescue clones that had lost OCT4 expression by 72 hr in both +LIF and −LIF, with or without doxycycline. Data are presented as mean ± standard deviation of triplicate experiments.

(G) Relative transcript levels of ESC-specific, self-renewal genes before and after long-term culture of rescue clones in doxycycline. Expression levels are reported as a percentage of expression in wild-type R1 cells. Data are presented as mean ± standard deviation of triplicate experiments.

Genome-wide Assessment of PCL2 Targets

To determine which genes were deregulated as a result of *Pcl2* knockdown, we performed expression microarray analysis. 2585 probes (1152 genes) (Table S2) were downregulated and 1715 probes (770 genes) (Table S2) were upregulated (Figure 5A) based on a fold-change cutoff of 1.5 and p value less than 0.05. Gene ontology (GO) analysis (Beissbarth and Speed, 2004) indi-

cated that upregulated genes are involved in transcription, chromatin remodeling, cell cycle, and DNA repair (Figure 5B) and included several key markers of undifferentiated ESCs. The majority of downregulated genes are involved in development and differentiation (Figure 5C).

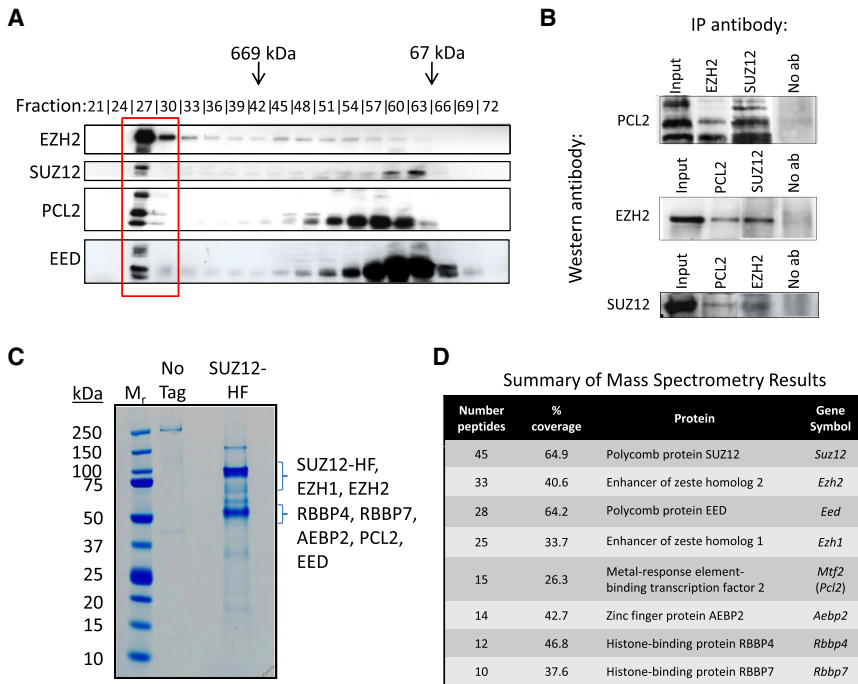To identify direct targets of PCL2, we performed ChIP-seq using a commercial antibody directed toward PCL2. The

A

669 kDa   67 kDa

Fraction: 21|24|27|30|33|36|39|42|45|48|51|54|57|60|63|66|69|72

EZH2
SUZ12
PCL2
EED

B

IP antibody:

Western antibody:

PCL2 — Input, EZH2, SUZ12, No ab

EZH2 — Input, PCL2, SUZ12, No ab

SUZ12 — Input, PCL2, EZH2, No ab

Figure 3. PCL2 is a PRC2-Associated Protein

(A) Gel filtration chromatography of ESC nuclear proteins indicating that PCL2, EED, and EZH2 coelute in the same fractions.

(B) Immunoblot analysis demonstrates that EZH2 and SUZ12 proteins are detected following IP with a PCL2-specific antibody. In addition, PCL2 protein is present following IP with an EZH2 antibody.

(C) Coomassie blue-stained gel of affinity-purified SUZ12 complex.

(D) Mass spectrometry results showing interaction of PCL2 with Suz12-HF.

C

kDa   M$_r$ No Tag   SUZ12-HF

250
150
100
75
50
37
25
20
15
10

SUZ12-HF, EZH1, EZH2
RBBP4, RBBP7, AEBP2, PCL2, EED

D

Summary of Mass Spectrometry Results

Number peptides	% coverage	Protein	Gene Symbol
45	64.9	Polycomb protein SUZ12	*Suz12*
33	40.6	Enhancer of zeste homolog 2	*Ezh2*
28	64.2	Polycomb protein EED	*Eed*
25	33.7	Enhancer of zeste homolog 1	*Ezh1*
15	26.3	Metal-response element-binding transcription factor 2	*Mtf2* (*Pcl2*)
14	42.7	Zinc finger protein AEBP2	*Aebp2*
12	46.8	Histone-binding protein RBBP4	*Rbbp4*
10	37.6	Histone-binding protein RBBP7	*Rbbp7*

in processes such as development, pattern specification, and differentiation (Figure 5F).

PCL2 Binds a Subset of PRC2 Targets and Is Associated with H3K27 Trimethylation at Those Targets

We have shown that PCL2 associates with PRC2; however, it is not clear whether PCL2 is present at all PRC2

antibody was first tested for specificity by overexpressing *Pcl2* in 293T cells (Figure S2A), as well as in the knockdown studies (Figures S2B and S2C). ChIP DNA was sequenced using the Solexa 1G platform, aligned to the mouse genome, and enrichment analysis was performed as described previously (Johnson et al., 2007), resulting in 3,847 enriched regions with a FDR of 0.3% (Table S3). Our analyses revealed that 47% of targets were within 100 kb of a known transcriptional start site (TSS) (Figure 5D) and 34%, or 1597 targets, were within 2 kb of a known TSS (Figure 5E). Further, GO analysis found that targets were involved

target locations. To identify specific targets regulated by the PCL2-PRC2 complex, we compared our ChIP-seq data to published ChIP-seq data sets for PRC2 components EZH2 and SUZ12 in mouse ESCs (Ku et al., 2008), as well as sites containing the histone modifications 3meH3K27 (catalyzed by PRC2) and 3meH3K4. This bivalent epigenetic mark occupies the promoters of developmental regulators in mouse ESCs (Bernstein et al., 2006; Ku et al., 2008). Finally, we incorporated the ChIP-seq data set for PRC1 component RING1B. Targets positive for both PRC2 and PRC1 binding are evolutionarily
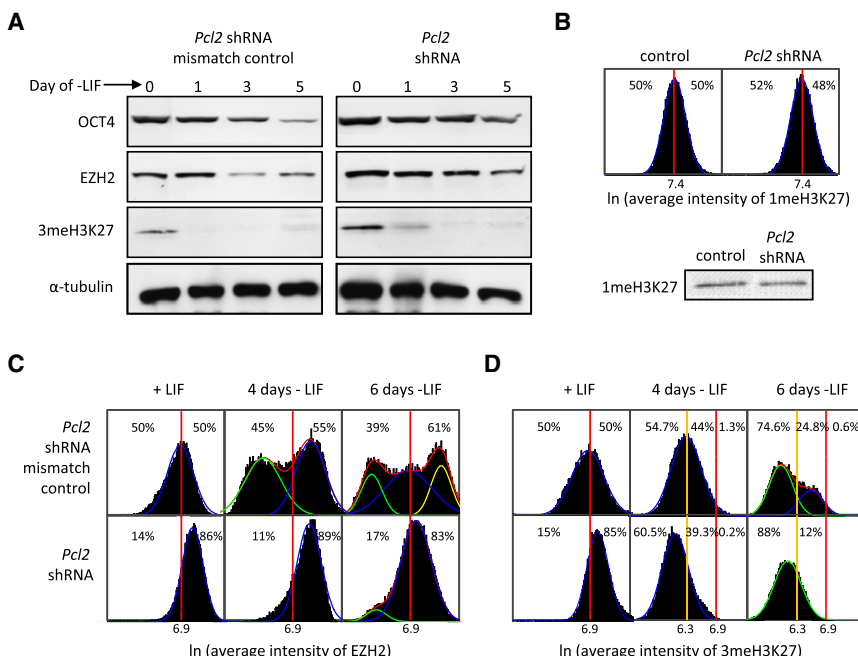
A

Pcl2 shRNA mismatch control   *Pcl2* shRNA

Day of -LIF → 0 1 3 5   0 1 3 5

OCT4
EZH2
3meH3K27
α-tubulin

B

control   *Pcl2* shRNA
50% | 50%   52% | 48%
7.4   7.4
ln (average intensity of 1meH3K27)

control   *Pcl2* shRNA
1meH3K27

Figure 4. PCL2 Knockdown Disrupts 3meH3K27 during Differentiation

(A) Immunoblot analysis demonstrates levels of OCT4, EZH2, and 3meH3K27 in *Pcl2* shRNA knockdown and mismatch control cells. α-tubulin was used as a loading control.

(B) H3K27 monomethylation levels in control versus knockdown.

(C and D) EZH2 (C) and 3me-H3K27 (D) protein was measured in 10,000 individual cells over 6 days in −LIF conditions. The distributions are best modeled as multipeak Gaussians (red curve) that are a compilation of the low population (green curve), midpopulation (blue curve), and high population (yellow curve).
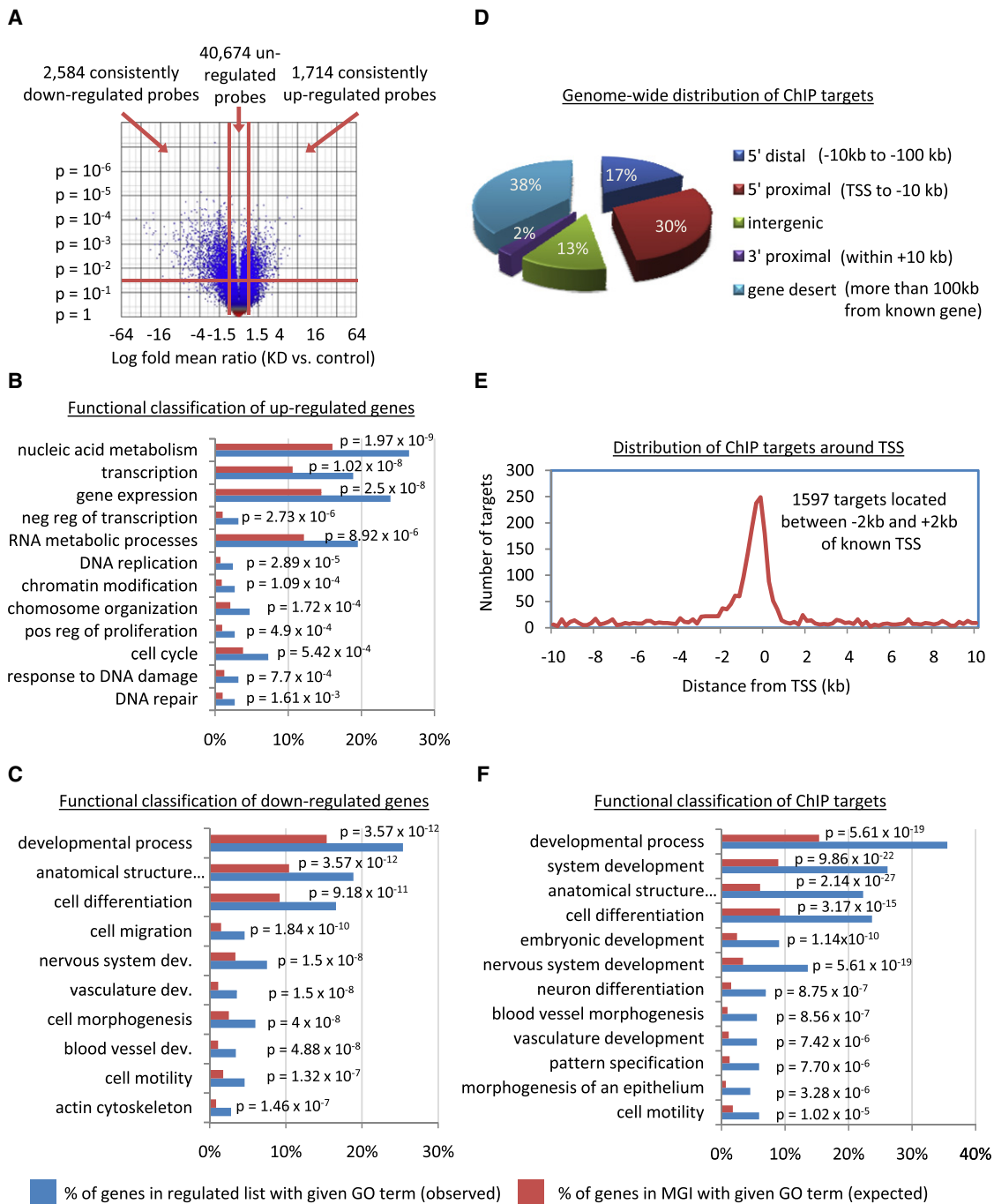
C

+ LIF   4 days - LIF   6 days -LIF

Pcl2 shRNA mismatch control
50%|50%   45%|55%   39%|61%

Pcl2 shRNA
14%|86%   11%|89%   17%|83%

6.9   6.9   6.9
ln (average intensity of EZH2)

D

+ LIF   4 days - LIF   6 days -LIF

50%|50%   54.7%|44%|1.3%   74.6%|24.8%|0.6%

15%|85%   60.5%|39.3%|0.2%   88%|12%

6.9   6.3 6.9   6.3 6.9
ln (average intensity of 3meH3K27)

Figure 5. Genome-wide Assessment of PCL2 Targets

(A) Volcano plot of differentially expressed genes between *Pcl2* shRNA knockdown cells and mismatch control cells cultured in +LIF. Vertical red line represents a fold change of ± 1.5. Microarrays were performed in triplicate, and the horizontal red line represents a cut-off p value of 0.05.

(B and C) GO analysis of genes upregulated and downregulated in knockdown cells.

(D) Location of enriched DNA sequence bound by PCL2 as determined by ChIP-seq.

(E) Histogram illustrating the distribution of enriched sequences in relation to known TSS.

(F) GO analysis illustrating the biological function GO terms overrepresented among the genes that were enriched in the ChIP-seq experiment. Statistically overrepresented GO terms were determined by comparing the incidence of a GO term within the input gene list (observed, red bar) to the incidence of that GO term among the entire mouse genome recorded in the MGI database (expected, yellow bar). Fisher's exact test was used to determine a p value for each term.

conserved and present on the majority of developmentally associated PRC2 targets (Ku et al., 2008).

By integrating these ChIP-seq data sets, we established that 953 were highly enriched for PCL2, EZH2, and SUZ12, and 96% of these targets were enriched for the bivalent domain (3meH3K27 + 3meH3K4) (Figure S3A and Table S3) and 65% were bound by RING1B. A second class of 772 targets was bound by EZH2 and SUZ12, but enrichment of PCL2 was below the 3-fold cutoff threshold. Comparable to the PCL2-PRC2 targets, 94% of these targets were enriched for the bivalent domain and 55% were bound by RING1B. The remaining subsets consisted of fewer targets and were not as likely to contain the bivalent domain or RING1B. Thus, PCL2 is highly enriched in a subset of PRC2 targets, and these targets are likely to be enriched for the bivalent domain as well as RING1B.

Figure 6A shows the aligned occupancy results of 14 genes whose expression was deregulated in the *Pcl2* knockdowns. *Oct4*, *Nanog*, and *Tcl1* were not bound by PCL2, or any of the PRC2 members, but were upregulated in the knockdowns. These genes are highly expressed in ESCs, consistent with exhibiting 3meH3K4, a well-validated transcriptional activation mark, but not 3meH3K27. Thus, these genes are likely to be indirectly inhibited by PCL2.

Tbx3 is also highly expressed in ESCs and was highly overexpressed in *Pcl2* knockdowns. Consistent with this, *Tbx3* exhibits the activating 3meH3K4 modification. Interestingly, it is also bound by PCL2, EZH2, and SUZ12 and has low levels of 3meH3K27. This suggests that *Tbx3* is controlled by PCL2-PRC2 through the modulation of 3meH3K27.

The remaining ten targets are developmental genes that were regulated in the *Pcl2* knockdowns. Overall, the binding profile of PCL2 shows remarkable overlap with the profiles of the other PRC2 members, strongly suggesting that they are binding to the same region of DNA.

ChIP-qPCR with antibodies directed against each PRC2 component was performed on 14 targets. Additionally, ChIP-qPCR was done on the knockdown cells to determine the effect of PCL2 depletion on PRC2 occupancy and 3meH3K27 at specific target promoters (Figures 6B–6F). 3meH3K27, as well as all PRC2 members, were enriched at these 11 targets. SUZ12 and EED enrichment were greatly reduced in the knockdown cells (Figures 6C and 6D), and EZH2 appeared less affected by loss of PCL2 (Figure 6E). Reduction in PCL2 expression does not disrupt the interactions of the core PRC2 components (Figure S3B). Finally, despite our observation that global 3meH3K27 was not depleted by loss of PCL2, we observed that 3meH3K27 enrichment was reduced by 2- to 3-fold in the *Pcl2* knockdown cells at these specific targets of PCL2 (Figure 6F). Collectively, these data are consistent with findings in *Drosophila* (Nekrasov et al., 2007) and suggest that PCL2 promotes PRC2 function at specific target, and despite being dispensable when assayed for global levels of 3meH3K27, PCL2 is required at *specific* PCL2-PRC2 targets to achieve proper 3meH3K27.

Our analysis also showed that PCL2 binds to a subset of 483 targets independently of PRC2. There is evidence that PCL2 can act as an activating transcription factor in mouse L-cells (Remondelli and Leone, 1997; Remondelli et al., 1997) and, thus, may function independently of PRC2 at some targets.

Upon further analysis, we found that most of these targets showed weak PCL2 enrichment and were not regulated following knockdown of *Pcl2*. Of the remaining 152 genes that were both bound and regulated, we then carefully analyzed the binding profiles of the other PRC2 members and found that, despite being below the cutoff threshold in the EZH2 and SUZ12 experiments, there was binding above background for nearly all. Ultimately, we identified a subset of 23 targets that appeared to be bound by PCL2 and not by other PRC2 proteins and that were also regulated following *Pcl2* knockdown. ChIP-qPCR at 11 of these targets confirmed that PCL2 was weakly bound in the wild-type cells and depleted in the knockdown cells (Figure S3C). EZH2 and 3meH3K27 were absent at these targets and were not altered following knockdown of *Pcl2* (Figures S3D–S3F). However, binding patterns of SUZ12 were remarkably similar to those of PCL2, and SUZ12 was displaced from these targets following knockdown of *Pcl2* (Figure S3D). Enrichment of SUZ12 at some of these targets (Figure S3D) suggests that they were false negatives in the SUZ12 ChIP-seq experiment. Together, these data suggest that if PCL2 regulates these targets, it may do so in cooperation with SUZ12 through a mechanism independent of 3meH3K27. However, with the exception of *Inhb1*, regulation following knockdown or overexpression is not significant (Figures S3H and S3I), and these targets are not regulated following the withdrawal of LIF (Figure S3H). It is possible that regulation of these targets is not critical in undifferentiated ESCs. It remains possible that PRC2 may play a role in regulating these targets in alternate cell types.

Predicting and Testing PCL2-Dependent ESC Regulatory Networks

To draft potential PCL2-PRC2-dependent ESC regulatory networks, we combined our ChIP-seq and microarray expression data with published ChIP-PET experiments for OCT4 and NANOG (Loh et al., 2006). The proximal promoter of *Pcl2* is bound by both OCT4 and NANOG, and because *Pcl2* is downregulated concomitantly with *Oct4* and *Nanog*, we reason that OCT4 and NANOG activate *Pcl2*. To extend the network, we incorporated our previously published time-course microarray data of differentiating ESCs (Walker et al., 2007). The complete network of 953 PCL2-PRC2 targets is summarized in Figure S4 and reveals that there is substantial overlap between the targets of OCT4, NANOG, and PCL2-PRC2. We found two distinct classes of targets. First, in the case of ESC-specific genes, OCT4 and NANOG exert an activating pressure that is opposed by the repressive effect of PCL2-PRC2. The interaction of three genes known to be important for ESC self-renewal (*Tbx3*, *Klf4*, and *Foxd3*) is highlighted in Figure 7A. The second class of OCT4, NANOG, and PCL2-PRC2 targets comprise developmental regulators that are directly repressed by PCL2-PRC2 (Figure 7B) but also repressed indirectly by OCT4 and NANOG through the activation of the extended pluripotency network (Figure S4).

To test the response of target genes immediately following perturbation of *Pcl2*, we used both transient siRNA and inducible overexpression. *Pcl2* transcript was depleted by 90% at 24 hr post-siRNA transfection, and target expression was elevated compared to the siRNA control by 72 hr (Figure 7C). Conversely,
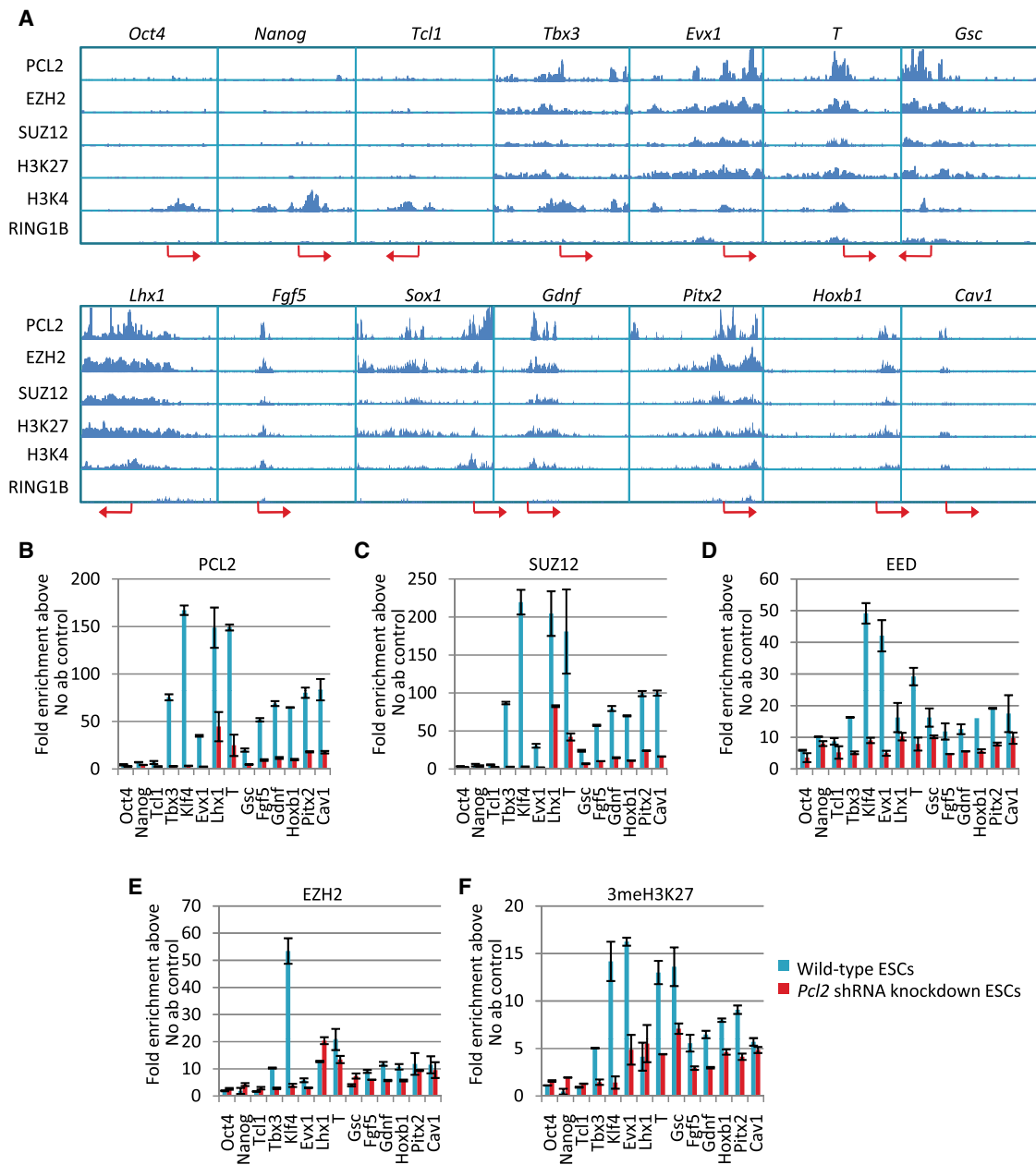
Figure 6. PCL2 Binds a Subset of PRC2 Targets and Is Associated with 3meH3K27

(A) Binding profiles of 14 PCL2 and PRC2 targets. Genomic range in each panel extends −10 kb from the TSS to the end of the gene.

(B–F) ChIP-qPCR validation of 14 selected promoter regions in both wild-type and knockdown cells for PCL2, EZH2, EED, SUZ12, and 3meH3K27. Values are calculated as the fold enrichment above a control without antibody. Wild-type versus knockdown samples were normalized to a fraction of the input material for each primer set tested to adjust for differences in starting amounts. Error bars represent the standard deviation of duplicate DNA samples. ChIP experiments were repeated three times, and comparable results were obtained for each experiment.

we used the aforementioned rescue clones to induce expression of *Pcl2* and observed that targets were decreased 72 hr after doxycycline treatment (Figure 7D).

In the case of the developmental genes, increased expression following transient siRNA (Figure 7C) is in contrast to the reduced expression of those same targets in the long-term culture of the *Pcl2* shRNA knockdown cells. We propose that this effect is due to increased repressive pressure on developmental targets exerted by the pluripotency network, which is overexpressed in the knockdown cells. Gene expression resulting from the long-term depletion of *Pcl2* is consistent with expression patterns of developmental targets in *Suz12* and *Ezh2* null ESCs (Pasini et al., 2007; Shen et al., 2008) (Figure 7E), although it is most similar to *Suz12* null cells.
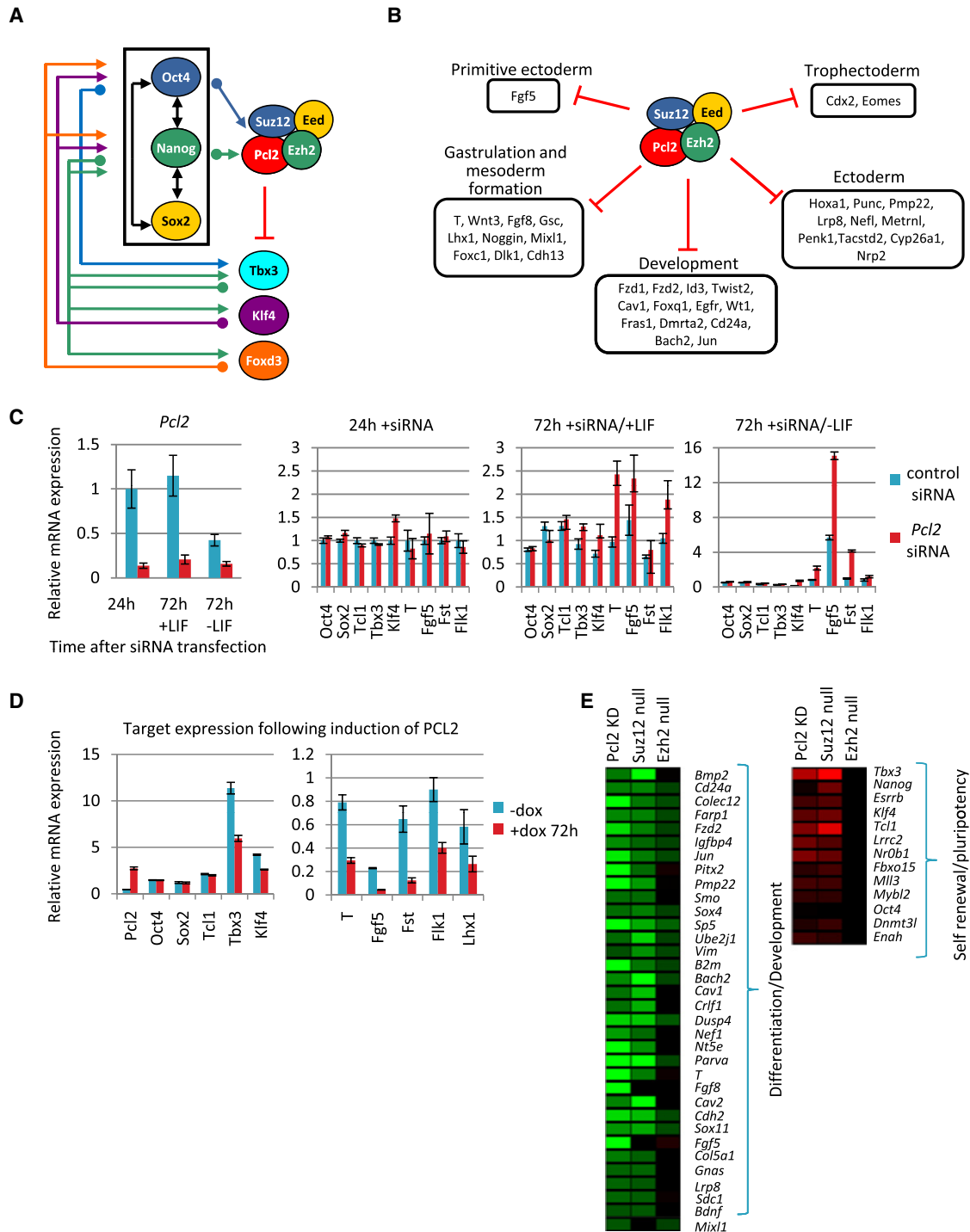
Figure 7. Predicting PCL2-Dependent Regulatory Networks

(A) Identification of one network motif that functions to modulate ESC pluripotency and self-renewal. Genes connected by an arrow were activated by the initiating gene, whereas genes connected by a T bar were repressed. Activation and repression is supported by promoter occupancy studies or microarray expression changes following knockdown.

(B) Summary of the categories of developmental genes found to be targeted by the PCL2-PRC2 complex.

(C) A pool of Dharmacon siRNAs targeting the *Pcl2* transcript were used to acutely knock down *Pcl2*. Cells were retransfected 48 hr after the first transfection to maintain depletion of *Pcl2*. Relative expression of *Pcl2*, as well as a set of potential targets, were measured 24 and 72 hr following transfection, in both +LIF and –LIF. Error bars represent the standard deviation of triplicate experiments.

(D) *Pcl2* expression was induced in the rescue clones, and transcript levels of the potential targets were measured 72 hr after doxycycline induction. Transcript levels are reported relative to their expression level in wild-type ESCs. Error bars represent the standard deviation of triplicate experiments.

(E) Microarray results from *Pcl2* knockdowns and *Suz12* and *Ezh2* null cells.

DISCUSSION

We predict that PCL2-PRC2 represses key members of the pluripotency network (Figures 7A and 7C–7E). Cells of the inner cell mass and ESCs, their in vitro derivatives, must undergo self-renewal while remaining poised to differentiate in response to extrinsic cues. Accumulated evidence suggests that ESCs maintain self-renewal through the autoregulation of the pluripotency TFs *Oct4*, *Nanog* and *Sox2*. In addition, some of the primary targets of these TFs, such as *Tbx3*, *Klf4* and *Foxd3*, support the pluripotency phenotype in part by stabilizing *Oct4*, *Nanog*, and *Sox2* through feedback mechanisms (Hanna et al., 2002; Ivanova et al., 2006; Kim et al., 2008). It has recently been shown that overexpression of either *Tbx3* or *Klf4* can support LIF-independent self-renewal (Niwa et al., 2009). Additionally, overexpression of *Klf4* can be used to revert adult fibroblasts to a pluripotent state and convert EpiSCs to ESCs (Guo et al., 2009; Takahashi and Yamanaka, 2006). Thus, it is likely that overexpression of *Tbx3* and *Klf4* due to depletion of PCL2 is a major determinant of the *Pcl2* knockdown phenotype, as predicted in our draft network (Figure 7A). Such a self-reinforcing network should result in a stable, self-renewing population of pluripotent stem cells.

However, experience reveals that even when grown under self-renewal culture conditions, a small but noticeable percentage of ESCs commit and undergo morphologically distinguishable differentiation. Furthermore, upon removal of LIF or induction of differentiation by addition of external signals such as retinoic acid, wild-type ESCs are able to rapidly downregulate these genes in response to external signals. We propose that PCL2 is critical for maintaining the capacity of ESCs to commit rather than self-renew by exerting repressive pressure on *Tbx3*, *Foxd3*, and *Klf4* through a feed-forward mechanism, thus dampening the autoregulatory network driving self-renewal to the point the cells can respond to external inputs (Figure 7A). Feed-forward motifs have been shown in bacteria to accelerate target response time and maintain steady-state levels of the target (Alon, 2007), and stabilization of transcript levels of *Tbx3*, *Foxd3*, and *Klf4* and indirectly of *Oct4*, *Nanog*, and *Sox2* through PCL2-PRC2 repression may be further beneficial to ESCs because it allows activation by a strong promoter, without risk of overshooting the optimal pluripotency TF concentration. Thus, one potential function of PCL2-PRC2 repression of ESC-specific genes is to allow rapid activation of the extended pluripotency network once the initiating TFs have been activated. Another potential function of PCL2-PRC2 repression is to regulate ESC fate by interrupting the self-reinforcing network that maintains pluripotency once the ESC is exposed to a differentiative environment.

Genome-wide promoter occupancy studies in ESCs have shown that EZH2, SUZ12, and EED also bind a large number of TFs required for development, leading to the hypothesis that PcG proteins maintain the ESC state by repressing developmental regulators that would otherwise cause the cells to differentiate (Boyer et al., 2006; Lee et al., 2006). However, knockdown and knockout studies of PcG proteins in ESCs have not supported this hypothesis. In the mouse, ablation of any of the three core PRC2 components does not result in embryonic lethality until the time of gastrulation (Faust et al., 1995; O'Carroll

et al., 2001; Pasini et al., 2004), and both *Suz12* and *Eed* null ESCs can be derived. *Suz12* null ESCs maintain an undifferentiated morphology and high levels of ESC markers even after withdrawal of self-renewal signals and are unable to differentiate into mature cell types (Pasini et al., 2007), which is similar to our findings for *Pcl2* knockdowns in ESCs. Additionally, *Eed* null ESCs express heightened levels of differentiation genes but also maintain high levels of ESC markers and can be taken to high passage without losing their undifferentiated morphology (Chamberlain et al., 2008). This suggests that PCL2-PRC2 and, in general, PRC2 target repression are not required to maintain the undifferentiated state. However, consistent with the established role of PRC2 in *Drosophila* gastrulation (Schuettengruber et al., 2007) and recent work implicating PcG in pattern formation (Oktaba et al., 2008), PCL2 depletion most dramatically affected PCL2-PRC2 target gene expression profiles during the early stages of ESC commitment to differentiation.

Despite the observed effect of PCL2 in modulating 3meH3K27 and PRC2 levels at its target promoters, we found that the integrity of the interactions between the core PRC2 components could still be observed in cell lysates from *Pcl2* knockdown cell lines. This could suggest that PCL2 is involved in the recruitment of the PRC2 complex, but not in its formation or stability.

It is counterintuitive to consider that *Pcl2* is both highly expressed in ESCs but required for repression of the self-renewal circuitry. The emerging landscape of the self-renewal regulatory network is of a dense and interconnected system of autoregulatory and feedback loops (Kim et al., 2008). We propose that one function of PCL2 is to provide the ESC with a mechanism to hold this system in check. Repression of self-renewal genes by *Tcf3* represents one other such ESC regulatory mechanism that has recently been identified (Yi et al., 2008). It will also be interesting to determine whether depletion of PCL2 will enhance the ability of adult cells to be reprogrammed into induced pluripotent stem cells (iPSCs). It is possible that the forced downregulation of PCL2 could result in hyperactivation of the self-renewal regulatory network, providing a selective advantage for reprogrammed cells.

EXPERIMENTAL PROCEDURES

ESC Culture

R1 ESCs were cultured as described previously (Walker et al., 2007).

shRNA Vector Design, Construction, and Electroporation

Three independent shRNA sequences were designed, cloned, and electroporated into R1 ESCs, and clones were derived as previously described (Walker et al., 2007). Mismatch controls were created by altering five of the 21 bases in the chosen *Pcl2* shRNA sequence. *Pcl2* target and mismatch sequences are provided in Supplemental Experimental Procedures.

Immunoprecipitation

R1 ESCs were pelleted and resuspended in co-IP lysis buffer. Two micrograms of antibody and 1 mg of total protein were combined, followed by immobilization with protein A/G beads (Pierce). The sample was separated from beads by centrifugation and run on a 15% SDS-PAGE for standard western blot analysis. Details of buffer solutions, antibody specifications, and western blot procedure are provided in Supplemental Experimental Procedures.

Protein Quantification in Single Cells

Cells were plated, cultured, stained, and imaged as described previously (Walker et al., 2007). Ten-thousand individual cells were imaged, and Gaussian

curves and statistics were generated using Origin 6.1 software. Additional details are provided in Supplemental Experimental Procedures.

Quantitative Real-Time PCR

Total RNA extraction and reverse transcription were performed as described (Walker et al., 2007). Serial dilutions of mouse genomic DNA were used to generate standard curves to adjust for the efficiency of each primer (Yun et al., 2006). Mouse genomic DNA standards or the cDNA template were added to the qPCR reaction in a final volume of 10 μl containing 2x SYBR master mix (Roche) and 0.5 μM primers. Standard Roche PCR protocol was performed on the Roche Light Cycler 480. qPCR primers are provided in Supplemental Experimental Procedures.

Clonogenic Assay and ALP Staining

Single-cell suspensions were plated in a 12-well dish at a density of 500 cells/well. Colonies were grown in +LIF for 5 days with media changed daily. ALP staining was performed as described previously (Walker et al., 2007).

Microarray Hybridizations

Total RNA was extracted from *Pcl2* mismatch controls and one *Pcl2* shRNA clone with RNeasy columns (QIAGEN). RNA quality was tested using an Agilent Bioanalyzer before performing standard cDNA synthesis (Invitrogen Superscript) and in vitro transcription (IVT) (Enzo IVT kit). Ten micrograms of RNA was used for IVT, and 15 μg of cRNA was used for hybridization (EukGE-WS2v4 kit) to the Mouse Genome 430 2.0 GeneChip. Scanning was performed using the Affymetrix GeneChip Scanner 3000 and analysis done using GCOS1.4 to obtain signal-log ratios of the control to the sample. Hybridizations of three biological replicates for both the control and *Pcl2* shRNA clone were performed.

ChIP-seq and ChIP-qPCR

DNA sonicated to approximately 1 kb lengths was supplied to The Centre for Applied Genomics (TCAG) for high-throughput sequencing or used for qPCR. Details of buffer solutions and qPCR primers are provided in Supplemental Experimental Procedures.

Generation of the HF-Tagged Allele of *Suz12*

An allele of *Suz12* encoding a full-length protein with a carboxy-terminal 3xFLAG-TEV-6xHis tag was created using a Cre recombinase-mediated modification of a gene trap allele. Briefly, we obtained an ESC line with a gene trap insertion in the seventh intron of the *Suz12* locus (XG122, Bay Genomics). Transient expression of Cre recombined Lox sites flanking the splice acceptor, and Cre-mediated recombination was also used to subsequently insert the coding sequence of the nine 3′ exons and tags.

Purification of Suz12-HF and Identification of Suz12-Interacting Proteins by Mass Spectrometry

Suz12-HF was purified according to the protocol of Andrew Krutchinsky (Deng et al., 2009). Modifications are noted in the Supplemental Experimental Procedures. After being separated by SDS-PAGE and stained with Coomassie blue (GelCode Blue, Pierce), protein bands were excised and processed for digestion with trypsin (Promega) as described (Shevchenko et al., 1996) and analyzed by LCMS.

Gel Filtration Chromatography

Nuclear protein extract was prepared from undifferentiated mouse ESCs as described by Dignam et al. (1983). Proteins (5 mg/ml) were separated by AKTA FPLC using a Superose 6 HR 10/30 gel filtration column (GE Healthcare). Approximately 1 mg of protein was loaded onto the column in a 50 mM Phosphate buffer containing 0.015 M NaCl (pH 7.0). Proteins were eluted at a flow rate of 0.4 ml/min in the same buffer, and 250 μl fractions were collected and analyzed by western blotting.

ACCESSION NUMBERS

Microarray data have been deposited at NCBI GEO under the accession number GSE16364. Raw ChIP-seq data has been deposited at NCBI GEO under the accession number GSE16526.

SUPPLEMENTAL INFORMATION

The Supplemental Information includes Supplemental Experimental Procedures, four figures, and three tables and can be found with this article online at doi:10.1016/j.stem.2009.12.014.

REFERENCES

Alon, U. (2007). Network motifs: theory and experimental approaches. Nat. Rev. Genet. *8*, 450–461.

Ambrosetti, D.C., Basilico, C., and Dailey, L. (1997). Synergistic activation of the fibroblast growth factor 4 enhancer by Sox2 and Oct-3 depends on protein-protein interactions facilitated by a specific spatial arrangement of factor binding sites. Mol. Cell. Biol. *17*, 6321–6329.

Beissbarth, T., and Speed, T.P. (2004). GOstat: find statistically overrepresented Gene Ontologies within a group of genes. Bioinformatics *20*, 1464–1465.

Bernstein, B.E., Mikkelsen, T.S., Xie, X., Kamal, M., Huebert, D.J., Cuff, J., Fry, B., Meissner, A., Wernig, M., Plath, K., et al. (2006). A bivalent chromatin structure marks key developmental genes in embryonic stem cells. Cell *125*, 315–326.

Boyer, L.A., Plath, K., Zeitlinger, J., Brambrink, T., Medeiros, L.A., Lee, T.I., Levine, S.S., Wernig, M., Tajonar, A., Ray, M.K., et al. (2006). Polycomb complexes repress developmental regulators in murine embryonic stem cells. Nature *441*, 349–353.

Cao, R., Wang, L., Wang, H., Xia, L., Erdjument-Bromage, H., Tempst, P., Jones, R.S., and Zhang, Y. (2002). Role of histone H3 lysine 27 methylation in Polycomb-group silencing. Science *298*, 1039–1043.

Chamberlain, S.J., Yee, D., and Magnuson, T. (2008). Polycomb repressive complex 2 is dispensable for maintenance of embryonic stem cell pluripotency. Stem Cells *26*, 1496–1505.

Chambers, I., Colby, D., Robertson, M., Nichols, J., Lee, S., Tweedie, S., and Smith, A. (2003). Functional expression cloning of Nanog, a pluripotency sustaining factor in embryonic stem cells. Cell *113*, 643–655.

Chambers, I., Silva, J., Colby, D., Nichols, J., Nijmeijer, B., Robertson, M., Vrana, J., Jones, K., Grotewold, L., and Smith, A. (2007). Nanog safeguards pluripotency and mediates germline development. Nature *450*, 1230–1234.

Czermin, B., Melfi, R., McCabe, D., Seitz, V., Imhof, A., and Pirrotta, V. (2002). *Drosophila* enhancer of Zeste/ESC complexes have a histone H3 methyltransferase activity that marks chromosomal Polycomb sites. Cell *111*, 185–196.

Davey, R.E., and Zandstra, P.W. (2006). Spatial organization of embryonic stem cell responsiveness to autocrine gp130 ligands reveals an autoregulatory stem cell niche. Stem Cells *24*, 2538–2548.

Deng, C., Xiong, X., and Krutchinsky, A.N. (2009). Unifying fluorescence microscopy and mass spectrometry for studying protein complexes in cells. Mol. Cell Proteomics. *8*, 1413–1423.

Dignam, J.D., Lebovitz, R.M., and Roeder, R.G. (1983). Accurate transcription initiation by RNA polymerase II in a soluble extract from isolated mammalian nuclei. Nucleic Acids Res. *11*, 1475–1489.

Duncan, I.M. (1982). Polycomblike: a gene that appears to be required for the normal expression of the bithorax and antennapedia gene complexes of *Drosophila melanogaster*. Genetics *102*, 49–70.

Evans, M.J., and Kaufman, M.H. (1981). Establishment in culture of pluripotential cells from mouse embryos. Nature *292*, 154–156.

Faust, C., Schumacher, A., Holdener, B., and Magnuson, T. (1995). The eed mutation disrupts anterior mesoderm production in mice. Development *121*, 273–285.

Furuyama, T., Tie, F., and Harte, P.J. (2003). Polycomb group proteins ESC and E(Z) are present in multiple distinct complexes that undergo dynamic changes during development. Genesis *35*, 114–124.

Guo, G., Yang, J., Nichols, J., Hall, J.S., Eyres, I., Mansfield, W., and Smith, A. (2009). Klf4 reverts developmentally programmed restriction of ground state pluripotency. Development *136*, 1063–1069.

Hanna, L.A., Foreman, R.K., Tarasenko, I.A., Kessler, D.S., and Labosky, P.A. (2002). Requirement for Foxd3 in maintaining pluripotent cells of the early mouse embryo. Genes Dev. *16*, 2650–2661.

Ivanova, N., Dobrin, R., Lu, R., Kotenko, I., Levorse, J., DeCoste, C., Schafer, X., Lun, Y., and Lemischka, I.R. (2006). Dissecting self-renewal in stem cells with RNA interference. Nature *442*, 533–538.

Johnson, D.S., Mortazavi, A., Myers, R.M., and Wold, B. (2007). Genome-wide mapping of in vivo protein-DNA interactions. Science *316*, 1497–1502.

Kaji, K., Caballero, I.M., MacLeod, R., Nichols, J., Wilson, V.A., and Hendrich, B. (2006). The NuRD component Mbd3 is required for pluripotency of embryonic stem cells. Nat. Cell Biol. *8*, 285–292.

Kim, J., Chu, J., Shen, X., Wang, J., and Orkin, S.H. (2008). An extended transcriptional network for pluripotency of embryonic stem cells. Cell *132*, 1049–1061.

Kim, H., Kang, K., and Kim, J. (2009). AEBP2 as a potential targeting protein for Polycomb Repression Complex PRC2. Nucleic Acids Res. *37*, 2940–2950.

Kitaguchi, T., Nakata, K., Nagai, T., Aruga, J., and Mikoshiba, K. (2001). Xenopus Polycomblike 2 (XPcl2) controls anterior to posterior patterning of the neural tissue. Dev. Genes Evol. *211*, 309–314.

Ku, M., Koche, R.P., Rheinbay, E., Mendenhall, E.M., Endoh, M., Mikkelsen, T.S., Presser, A., Nusbaum, C., Xie, X., Chi, A.S., et al. (2008). Genomewide analysis of PRC1 and PRC2 occupancy identifies two classes of bivalent domains. PLoS Genet. *4*, e1000242. 10.1371/journal.pgen.1000242.

Kunath, T., Gish, G., Lickert, H., Jones, N., Pawson, T., and Rossant, J. (2003). Transgenic RNA interference in ES cell-derived embryos recapitulates a genetic null phenotype. Nat. Biotechnol. *21*, 559–561.

Kuzmichev, A., Nishioka, K., Erdjument-Bromage, H., Tempst, P., and Reinberg, D. (2002). Histone methyltransferase activity associated with a human multiprotein complex containing the Enhancer of Zeste protein. Genes Dev. *16*, 2893–2905.

Kuzmichev, A., Margueron, R., Vaquero, A., Preissner, T.S., Scher, M., Kirmizis, A., Ouyang, X., Brockdorff, N., Abate-Shen, C., Farnham, P., and Reinberg, D. (2005). Composition and histone substrates of polycomb repressive group complexes change during cellular differentiation. Proc. Natl. Acad. Sci. USA *102*, 1859–1864.

Lee, T.I., Jenner, R.G., Boyer, L.A., Guenther, M.G., Levine, S.S., Kumar, R.M., Chevalier, B., Johnstone, S.E., Cole, M.F., Isono, K., et al. (2006). Control of developmental regulators by Polycomb in human embryonic stem cells. Cell *125*, 301–313.

Loh, Y.H., Wu, Q., Chew, J.L., Vega, V.B., Zhang, W., Chen, X., Bourque, G., George, J., Leong, B., Liu, J., et al. (2006). The Oct4 and Nanog transcription network regulates pluripotency in mouse embryonic stem cells. Nat. Genet. *38*, 431–440.

Lund, A.H., and van Lohuizen, M. (2004). Polycomb complexes and silencing mechanisms. Curr. Opin. Cell Biol. *16*, 239–246.

Martin, G.R. (1981). Isolation of a pluripotent cell line from early mouse embryos cultured in medium conditioned by teratocarcinoma stem cells. Proc. Natl. Acad. Sci. USA *78*, 7634–7638.

Mitsui, K., Tokuzawa, Y., Itoh, H., Segawa, K., Murakami, M., Takahashi, K., Maruyama, M., Maeda, M., and Yamanaka, S. (2003). The homeoprotein Nanog is required for maintenance of pluripotency in mouse epiblast and ES cells. Cell *113*, 631–642.

Morrison, G.M., and Brickman, J.M. (2006). Conserved roles for Oct4 homologues in maintaining multipotency during early vertebrate development. Development *133*, 2011–2022.

Nekrasov, M., Klymenko, T., Fraterman, S., Papp, B., Oktaba, K., Köcher, T., Cohen, A., Stunnenberg, H.G., Wilm, M., and Müller, J. (2007). Pcl-PRC2 is needed to generate high levels of H3-K27 trimethylation at Polycomb target genes. EMBO J. *26*, 4078–4088.

Nichols, J., Zevnik, B., Anastassiadis, K., Niwa, H., Klewe-Nebenius, D., Chambers, I., Schöler, H., and Smith, A. (1998). Formation of pluripotent stem cells in the mammalian embryo depends on the POU transcription factor Oct4. Cell *95*, 379–391.

Niwa, H., Miyazaki, J., and Smith, A.G. (2000). Quantitative expression of Oct-3/4 defines differentiation, dedifferentiation or self-renewal of ES cells. Nat. Genet. *24*, 372–376.

Niwa, H., Ogawa, K., Shimosato, D., and Adachi, K. (2009). A parallel circuit of LIF signalling pathways maintains pluripotency of mouse ES cells. Nature *460*, 118–122.

O'Carroll, D., Erhardt, S., Pagani, M., Barton, S.C., Surani, M.A., and Jenuwein, T. (2001). The polycomb-group gene Ezh2 is required for early mouse development. Mol. Cell. Biol. *21*, 4330–4336.

O'Connell, S., Wang, L., Robert, S., Jones, C.A., Saint, R., and Jones, R.S. (2001). Polycomblike PHD fingers mediate conserved interaction with enhancer of zeste protein. J. Biol. Chem. *276*, 43065–43073.

Oktaba, K., Gutierrez, L., Gagneur, J., Girardot, C., Sengupta, A.K., Furlong, E.E., and Muller, J. (2008). Dynamic regulation by polycomb group protein complexes controls pattern formation and the cell cycle in *Drosophila*. Dev. Cell *15*, 877–889.

Pasini, D., Bracken, A.P., Jensen, M.R., Lazzerini Denchi, E., and Helin, K. (2004). Suz12 is essential for mouse development and for EZH2 histone methyltransferase activity. EMBO J. *23*, 4061–4071.

Pasini, D., Bracken, A.P., Hansen, J.B., Capillo, M., and Helin, K. (2007). The polycomb group protein Suz12 is required for embryonic stem cell differentiation. Mol. Cell. Biol. *27*, 3769–3779.

Peerani, R., Bauwens, C., Kumacheva, E., and Zandstra, P.W. (2009). Patterning mouse and human embryonic stem cells using micro-contact printing. Methods Mol. Biol. *482*, 21–33.

Remondelli, P., and Leone, A. (1997). Interactions of the zinc-regulated factor (ZiRF1) with the mouse metallothionein Ia promoter. Biochem. J. *323*, 79–85.

Remondelli, P., Moltedo, O., and Leone, A. (1997). Regulation of ZiRF1 and basal SP1 transcription factor MRE-binding activity by transition metals. FEBS Lett. *416*, 254–258.

Rodda, D.J., Chew, J.L., Lim, L.H., Loh, Y.H., Wang, B., Ng, H.H., and Robson, P. (2005). Transcriptional regulation of nanog by OCT4 and SOX2. J. Biol. Chem. *280*, 24731–24737.

Savla, U., Benes, J., Zhang, J., and Jones, R.S. (2008). Recruitment of *Drosophila* Polycomb-group proteins by Polycomblike, a component of a novel protein complex in larvae. Development *135*, 813–817.

Schuettengruber, B., Chourrout, D., Vervoort, M., Leblanc, B., and Cavalli, G. (2007). Genome regulation by polycomb and trithorax proteins. Cell 128, 735–745.

Schwartz, Y.B., and Pirrotta, V. (2007). Polycomb silencing mechanisms and the management of genomic programmes. Nat. Rev. Genet. 8, 9–22.

Shen, X., Liu, Y., Hsu, Y.J., Fujiwara, Y., Kim, J., Mao, X., Yuan, G.C., and Orkin, S.H. (2008). EZH1 mediates methylation on histone H3 lysine 27 and complements EZH2 in maintaining stem cell identity and executing pluripotency. Mol. Cell 32, 491–502.

Shevchenko, A., Wilm, M., Vorm, O., and Mann, M. (1996). Mass spectrometric sequencing of proteins silver-stained polyacrylamide gels. Anal. Chem. 68, 850–858.

Silva, J., Mak, W., Zvetkova, I., Appanah, R., Nesterova, T.B., Webster, Z., Peters, A.H., Jenuwein, T., Otte, A.P., and Brockdorff, N. (2003). Establishment of histone h3 methylation on the inactive X chromosome requires transient recruitment of Eed-Enx1 polycomb group complexes. Dev. Cell 4, 481–495.

Singla, V., Hunkapiller, J., Santos, N., Seol, A.D., Norman, A.R., Wakenight, P., Skarnes, W.C., and Reiter, J.F. (2010). Floxin, a resource for genetically engineering mouse ESCs. Nat. Methods 7, 50–52.

Smith, A.G., and Hooper, M.L. (1987). Buffalo rat liver cells produce a diffusible activity which inhibits the differentiation of murine embryonal carcinoma and embryonic stem cells. Dev. Biol. 121, 1–9.

Smith, A.G., Heath, J.K., Donaldson, D.D., Wong, G.G., Moreau, J., Stahl, M., and Rogers, D. (1988). Inhibition of pluripotential embryonic stem cell differentiation by purified polypeptides. Nature 336, 688–690.

Takahashi, K., and Yamanaka, S. (2006). Induction of pluripotent stem cells from mouse embryonic and adult fibroblast cultures by defined factors. Cell 126, 663–676.

Tie, F., Prasad-Sinha, J., Birve, A., Rasmuson-Lestander, A., and Harte, P.J. (2003). A 1-megadalton ESC/E(Z) complex from Drosophila that contains polycomblike and RPD3. Mol. Cell. Biol. 23, 3352–3362.

Walker, E., Ohishi, M., Davey, R.E., Zhang, W., Cassar, P.A., Tanaka, T.S., Der, S.D., Morris, Q., Hughes, T.R., Zandstra, P.W., et al. (2007). Prediction and testing of novel transcriptional networks regulating embryonic stem cell self-renewal and commitment. Cell Stem Cell 1, 71–86.

Wang, S., Yu, X., Zhang, T., Zhang, X., Zhang, Z., and Chen, Y. (2004). Chick Pcl2 regulates the left-right asymmetry by repressing Shh expression in Hensen's node. Development 131, 4381–4391.

Wang, S., He, F., Xiong, W., Gu, S., Liu, H., Zhang, T., Yu, X., and Chen, Y. (2007). Polycomblike-2-deficient mice exhibit normal left-right asymmetry. Dev. Dyn. 236, 853–861.

Williams, R.L., Hilton, D.J., Pease, S., Willson, T.A., Stewart, C.L., Gearing, D.P., Wagner, E.F., Metcalf, D., Nicola, N.A., and Gough, N.M. (1988). Myeloid leukaemia inhibitory factor maintains the developmental potential of embryonic stem cells. Nature 336, 684–687.

Woltjen, K., Michael, I.P., Mohseni, P., Desai, R., Mileikovsky, M., Hämäläinen, R., Cowling, R., Wang, W., Liu, P., Gertsenstein, M., et al. (2009). piggyBac transposition reprograms fibroblasts to induced pluripotent stem cells. Nature 458, 766–770.

Yi, F., Pereira, L., and Merrill, B.J. (2008). Tcf3 functions as a steady-state limiter of transcriptional programs of mouse embryonic stem cell self-renewal. Stem Cells 26, 1951–1960.

Ying, Q.L., Nichols, J., Chambers, I., and Smith, A. (2003a). BMP induction of Id proteins suppresses differentiation and sustains embryonic stem cell self-renewal in collaboration with STAT3. Cell 115, 281–292.

Ying, Q.L., Stavridis, M., Griffiths, D., Li, M., and Smith, A. (2003b). Conversion of embryonic stem cells into neuroectodermal precursors in adherent monoculture. Nat. Biotechnol. 21, 183–186.

Yuan, H., Corbi, N., Basilico, C., and Dailey, L. (1995). Developmental-specific activity of the FGF-4 enhancer requires the synergistic action of Sox2 and Oct-3. Genes Dev. 9, 2635–2645.

Yun, J.J., Heisler, L.E., Hwang, I.I., Wilkins, O., Lau, S.K., Hyrcza, M., Jayabalasingham, B., Jin, J., McLaurin, J., Tsao, M.S., and Der, S.D. (2006). Genomic DNA functions as a universal external standard in quantitative real-time PCR. Nucleic Acids Res. 34, e85.

Zhang, W., Walker, E., Tamplin, O.J., Rossant, J., Stanford, W.L., and Hughes, T.R. (2006). Zfp206 regulates ES cell gene expression and differentiation. Nucleic Acids Res. 34, 4780–4790.